Proceedings of CONF-CIAP 2026 Symposium: International Conference on Atomic Magnetometer and Applications
DOI: 10.54254/2753-8818/2026.HZ30775

Alternative Method for Energy Harvesting — A Study of Water Wave Control Using Metasurfaces

Ziqing Liu

Shanghai Pinghe Bilingual School, Shanghai, China
daylight_901003@126.com

Abstract. Among all the rapidly growing global demand for electrical energy, a disturbing conundrum exhibits itself in growing numbers; nature inevitably wastes its inconceivable amounts of energy, while humans struggle to produce electricity from fossil fuels. This research investigates the practicability of employing energy stored in the ceaseless oscillations of water waves on the surface of the water bodies. Since water waves are largely chipped away by continental slopes as they approach near-land regions, this research designed and tested a method to concentrate them for their collection. Drawing insight from Extended Snell's Law and metasurfaces in Transformational Optics, the researcher used calculations based on existing research to build a metasurface with rigorously designed refractive indices, producing an anisotropic reflective surface that converges water waves just like convex lens converges visible light. With the purpose of making light incur different phases, the mechanical method have been proven effective by simulation: adjoining units varying light path, so as to create a change in effective refractive index. Completing original work from theoretical deductions, designing, modelling, simulations and finally experiments, this research confirmed the success of the lens in wave focusing. Despite limited results given the small physical scale of the experimental setup, the researcher believed the methods of designing and modelling are worthy of greater application.

Keywords: Metasurface, water wave focusing, Extended Snell's Law, electrical energy harvesting

1. Introduction

Energy sustainability is one of most concerning topics in modern technology development [1].Global energy consumption was more than 51,000 terawatt-hours (TWh) in 2024, according to an International Energy Agency Report [2]. Yet only around 30% of the total energy consumption is produced by renewable energy, in which hydropower accounts for almost half of this production [3]. While most hydraulic electricity plants rely on an elevational discrepancy, the researcher is more interested into harnessing another incessant movement of water – waves and tides.Another benefit from the utilisation of water wave energy is to prevent destructive outcomes they may originally develop into. Statistics from a United Nations tally, the world has incurred over 280 billion US dollars of cost due to damages caused by tsunamis, for the decade 2009-2018 [4]. Fore by, more than 1 million large and medium-sized ships and more than 60 offshore oil platforms have been struck

DOI: 10.54254/2753-8818/2026.HZ30775

down by high waves and wind [5]. Water wave control would be a way of directing this energy that was now destructive into useful ways.

Attempts on using water wave energy to generate electricity highlight another structural barrier to efficient water wave energy capturing: While energy-effective waves are only generated in the distant sea hundreds of kilometres away from the shore, the rising of the ocean bed sharply attenuates the energy of the waves near the shore. Therefore, the proposition for the field of water wave energy is clear: If, by artificial means, can water waves be gathered collectively, how much energy can be useful output?

By analogizing ocean waves to light waves, the construction of a sort of "wave lens" along the coast that "focuses" large waves for efficient electricity generation. Metasurfaces utilize periodic microstructures of subwavelength size to phase-modulate waves and manipulate their propagation direction, which has the advantages of compact size and high controllability [6]. Currently, optical and acoustic manipulation based on hypersurface structures has enabled applications such as stealth suits and acoustic cloaks [7] by manipulating wave propagation trajectories [8,9]. Based on this idea, we will design the metasurface surface from the basic theory, simulate and optimize its water wave convergence characteristics; meanwhile, we will fabricate a highly efficient nanogenerator and apply it to the water wave power generation, and finally build a systematic solution that takes both wave protection and green power generation into account.

2. Literature review

In response to the difficulties in utilising wave energy, researchers have proposed the use of metasurfaces to gather waves to specific locations for efficient power generation. Existing research is evaluated centring from this aim.

2.1. Metasurfaces

The term "transformational optics" refers to the practice of controlling linear liquid surface waves, namely water waves, to enhance or attenuate by transforming theoretical properties of the medium. This model outlines theoretical groundwork for the mechanism through which subjective modulations on the shape of the container or the flow speed can achieve effects such as bending, focusing, circumventing and waveguide. The transformational medium parameters such as refractive index can be controlled by equivalents such as depth and flow velocity distribution. Through theoretical modelling and simulations, the propagation direction of surface waves can be precisely manipulated by adjusting the geometric characteristics the liquid. Several studies have explored how to utilize metasurfaces to manipulate the propagation of water waves.

Relative early takings to wave manipulation have highlighted achievements in the proposition of the concept of anisotropic depths so as to achieve invisible water wave concentrators [10]. Extending from electromagnetism, the wave rotator created anisotropic depth around the rotator. Because anisotropic depth corresponds to anisotropic permittivity, the patter of water wave propagation can be altered. Experimental setups on anisotropic depths have evolved to prove the effectiveness of a gradient refractive indices lens in manipulating planar waves [11-14]. On these groundworks, successful outcomes are produced by respective devices in bending, directional emissions and focusing [15]. Further introducing the gradient depth profile into Fabry-Perot resonances, an effectively invisible wave amplifier was developed [16,17] Using the relationship that the wavelength is the half-integer multiple of the distance travelled, each slit can completely eliminate destructive interference caused by reflection, so as to augment the original wave shape.

DOI: 10.54254/2753-8818/2026.HZ30775

Alternatively, Bonbinski et al [18] explored how to utilize the concept of epsilon-near-zero (ENZ) materials to enhance the efficiency of effective focusing of water waves from the viewpoint of material properties. Their design of an ENZ lens (Figure 1) was very contributing and insightful, but their method has its limitations because the research construed a sudden change in water depth and a large, continuous arc structure is unrealistic in this research's hypothetical scene.

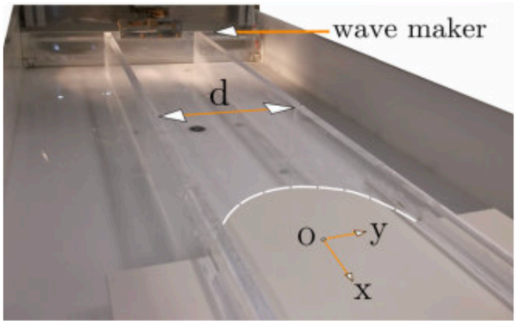

Figure 1. Lens made from ENZ material [19]

On the other hand, other research has explored the practicability of extending surface plasmons properties in optical and acoustic manipulation to water waves, namely rainbow trapping [18-20]. By using a line-up of wave-flume arrays with spacing increasing in the incident wave direction, rainbow trapping has been observed to be amplify different wavelengths at discrete positions, effectively separating wavelengths in broadband waves [21].

Taking theoretical grounds from constructing anisotropic permittivity, the researcher combined that with the spatial design of a converging lens. In making a reflection surface anisotropic in terms of its refractive index, the path of the light can bend with a gradual gradient change so as to finally converge into focus point. Since most of the review literature employed mathematically rigorous designs on a gradient water depth, so as to cause anisotropic distribution of the refractive index and phases, the researcher probed one design of metasurface that shifts the phase directly by mechanical means. This would be described in detail in section 4; namely, the researcher designed compartments with anisotropic light paths to give them different refractive index and phases. The researcher also continued the design in the fashion of gradient depths for their effective elimination of unwanted reflection, included in the discussion section.

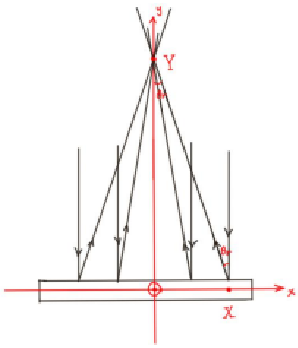

Figure 2. Diagram what the researcher envision as the wave amplifying lens

DOI: 10.54254/2753-8818/2026.HZ30775

2.2. Generating electricity

The second proposition in this research is how to efficiently convert mechanical water wave energy into electrical energy. Although the common-sense turbine structure achieves this by carrying water wave energy into a rotational motion, the structure is inefficient and lack flexibility. In contrast, nanogenerators are an emerging energy conversion device with the advantages of compact structure and high energy conversion efficiency. According to different mechanisms, nanogenerators can be categorized into triboelectric nanogenerators (TENG) and piezoelectric nanogenerators (PENG).

PENGs are designed to generate an electric current through the change of dipoles on the surface of a piezoelectric material. When the material is subjected to an external force (compression or stretching), there is a relative displacement between the centre for positive and negative charges inside the crystal, whose separation is used to generate electricity. Unlike TENGs, PENGs directly utilize the piezoelectric effect of materials, so the choice of materials with piezoelectricity are crucial to its performance [22-24] Compounds with highly asymmetric electric negativity, such as GaN [25] and ZnO [26] are often considered.

PENGs rely on the piezoelectric effect of the material itself, so enhancing the efficiency of their power generation can be clearly focused on increasing the nanomaterials' geometrical structure, thermal stability and piezoelectric coefficients, etc [27]. In order to obtain the desired characteristics. The output voltage and current of PENGs are not significantly affected by large variations in the environment, giving it a major advantage over friction nanogenerators.

3. Theoretical background

3.1. Transformational optics and meta-surfaces

Meta-surfaces are periodic structures in a scale remarkably smaller than the wavelength of the wave. An optical metasurface can dictate the direction of the transmitted or reflected light by creating a phase gradient at the interface, creating interesting phenomenon like negative or zero refractive indices and transformation optics cloaking. When an abrupt change in the refractive index occurs, the extended Snell's Law in reflective conditions can be applied [28]:

$$\sin(\theta_t) - \sin(\theta_i) = \frac{\lambda_0}{2\pi n_1}\frac{d\phi(x)}{dx} \tag{1}$$

where $\frac{d\phi(x)}{dx}$ is the rate of change of the phase. Meta-surfaces utilise the correspondence between material parameters and coordinate transformations of the permittivity tensor and the permeability tensor. Using methods from previous research,the model of water waves in an x-y plane can be modelled by Equation (4): (considering a depth tensor u)

$$\nabla \bullet (u\nabla p) + \frac{\omega^2}{g}p = 0 \tag{2}$$

By comparing (4) to the transverse magnetic mode of Maxwell's equations would give:

$$H_z \leftrightarrow p,\ \frac{1}{\varepsilon_y\varepsilon_0} \leftrightarrow u_x,\ \frac{1}{\varepsilon_x\varepsilon_0} \leftrightarrow u_y,\ \frac{1}{\mu\mu_0} \leftrightarrow g \tag{3}$$

By defining a depth tensor u = tanh(k h)/k to describe the refractive index distribution, we can make the refractive index also a function of water depth. This is because the angular frequency ω of

DOI: 10.54254/2753-8818/2026.HZ30775

dispersion in water waves is described as a function of water depth h,

$$\omega = \sqrt{\left(gk + \frac{T^3}{\rho} k^3\right) \tanh(kh)} \tag{4}$$

k=2π/λ is the wawvenumber, p=ρgη is the hydrostatic pressure at the water surface.

3.2. Energy harvesting

To convert the mechanical energy of water waves into electric energy, various types of wave energy generators have been developed. Compared with the existing technologies, the nanogenerators feature compact size and low cost, making it a promising path toward water wave energy harvesting. Both triboelectric nanogenerators (TENG) and PENGs (PENG) can convert mechanical energy to electrical energy [29]. TENGs rely on a periodically recurring process of contact electrification and subsequent separation between two materials [30,31]. An imbalance of charges is created on the two plates respectively, generating a potential difference that gives charges the tendency to move from one side to the other. Thus, an alternative current is created through the mechanical energy forcing the plates into and out of contact. PENGs rely on the piezoelectric effect, in which a mechanical stress produces electrical charges in a material; in reverse, an electrical field produces physical deformation. When a mechanical energy is raised in a piezoelectric material, its molecular arrangement of dipoles alters to give discrete deflections between positive and negative charges [32]. As mechanical forces cause the charges to line up in both directions, an alternative current is also generated from PENGs.

4. Modelling and simulation

To efficiently harvest the wave energy, it is essential to firstly develop a metasurface that can effectively focus water waves. A schematic of the theoretical model is presented in Figure 3. The incident planar water waves are reflected by the bank with metasurfaces and are focused at a distance of Y(0, Y). The reflection at the bank is subjected by the extended Snell's law for reflections.

$$\sin(\theta_t) - \sin(\theta_i) = \frac{\lambda_0}{2\pi n_i} \frac{d\phi(x)}{dx} \tag{5}$$

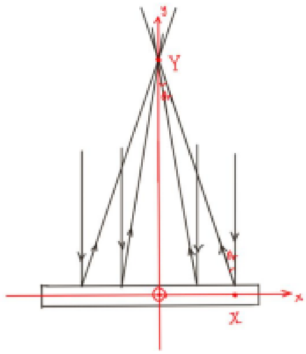

Figure 3. Diagram of the mechanism of the wave amplifying lens. (X,0) is the point of incidence, and Y is the focus

DOI: 10.54254/2753-8818/2026.HZ30775

In this scenario, the refraction index n_i is set to be 1, and since the incident ray is perpendicular to the structure, $sin\,(\theta_i)$ =0.

$$-\frac{X}{\sqrt{X^2+Y^2}} = \frac{\lambda_0}{2\pi}\frac{d\phi(x)}{dx} \tag{6}$$

After solving and rearranging:

$$\phi = \frac{2\pi}{\lambda}\left(\sqrt{X^2+Y^2} - Y\right) + \phi_0 \tag{7}$$

Assumptions:

Before the article delves into the specific designs that manipulates the waves, the assumptions should be priorly stated.

1. If the water depth is set at 0.2 m, then v = 1.4 m/s.
2. If the frequency of the wave is set at 10 Hz, then λ is 0.14m.
3. If the researcher wants the reflection rays to converge at 1 m away from the meta-structure (0, Y) , a phase difference of 2π would require a 0.54736m displacement in the x direction.

$$0.54736\text{m} \equiv 2\pi \tag{8}$$

For the convenience of calculation, calculations would only consider when y>0 based on mirror symmetry. Therefore, the greater X, the smaller the effective path, the smaller the refractive index.

4.1. Maze design

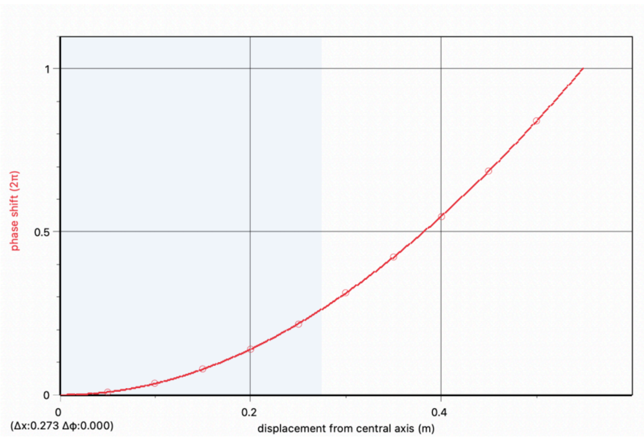

Figure 4. Phase shift v. displacement from central axis (ϕ v. x) graph, visual representation of Equation (8). As shown in the blue region, at point (0.274, 0.26139), ϕ ≈0.52278π, which means there is only about a quarter of a complete period

For all path lengths (l) it is measured in metres (m)

$$l = 2(0.003 + \sqrt{0.023^2 + (b - 0.020)^2} + 0.003 + \sqrt{0.023^2 + b^2}) \tag{9}$$

where in equation (18), b is the length of the barrier plate (m). Where φ is phase change (2π) and λ is wavelength (m).

DOI: 10.54254/2753-8818/2026.HZ30775

For the calculation of the length of the barrier plate, see Appendix 1. For the convenience of calculations, $\frac{0.055}{2} \approx 0.023m$. The thickness for all the boundaries is set at 0.003m, and each opening is left at 0.020m.

This set of assumed conditions give, phase change = 2.921931π

$$0.052 \equiv 2.921931\pi \tag{10}$$

where b=0.052, As the initial conditions

Table 1. Calculation of the respective phase shifts the researcher should be looking for using a total displacement of 0.274m in the x direction

Unit length of meta-structure (m)	Number of units	Displacement (m)	phase shift (2π)	phase shift (π)	Relative phase shift(π)
		= unit length * number	Eq.(8)		
0.068	1	0.068	0.016495239	0.032990478	2.888941
0.068	2	0.136	0.065754487	0.131508974	2.790422
0.068	3	0.204	0.147113603	0.294227205	2.627704

Focusing on the results obtained in the right most column in Table 1, the barrier lengths that produce phase shifts closest to the last column of Table 1 were extracted.

These data from Appendix 1 has been provided as following:

Table 2. The working by which the lengths of the barriers are determined

Frequency (Hz)	Wave speed (m/s)	Barrier length (m)	Relative Path length (m)	Phase change (2π)	Phase change (π)	note
		b	Eq. (18)	= path length/ wavelength		
10	1.4	0.052	0.204535	1.460966	2.921931	Identity (20)
10	1.4	0.0513	0.202124	1.443741	2.887482	
10	1.4	0.0493	0.1953	1.395003	2.790006	
10	1.4	0.0458	0.183629	1.311633	2.623266	

Using data from Table 2, the following design diagrams were illustrated.

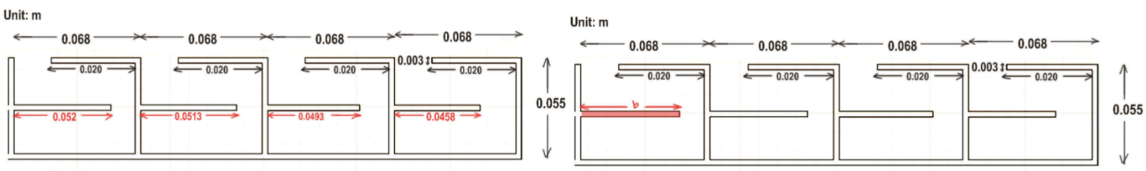

Figure 5. The design for the maze metasurface on the positive x-axis

DOI: 10.54254/2753-8818/2026.HZ30775

4.2. Simulations

Using the design in Figure 6, the complete structure is obtained by mirroring the demonstrated half across the leftmost vertical side. Importing the structure for simulations based on acoustic pressure scenarios, the focusing effects of the structure is demonstrated.

In this model, Acoustic waves are equivalent to water waves and the only parameter that needs modification is wave speed; as assumed, it is 1.4 m/s. As acoustic pressure (acpr.) is the representation of acoustic wave intensity, it shall equally serve to denote water wave intensity. The darker the colour of the region is, the stronger the wave is. Total acoustic pressure is the result of superposition of the incoming background water waves in the -y direction and the reflected water waves in the +y direction.

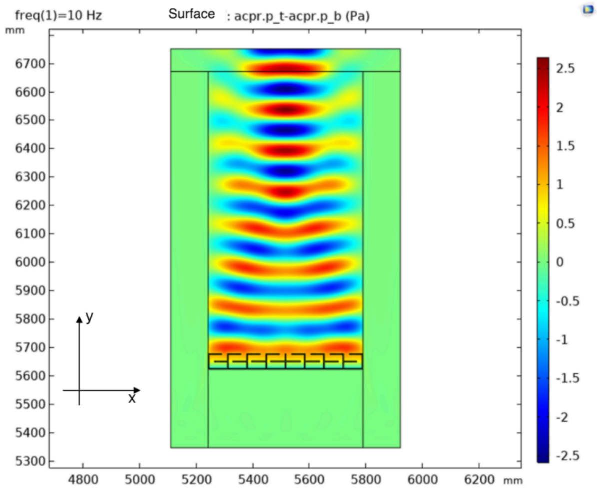

Figure 6. The simulation results produced using COMSOL Multiphysics

With the base of metasurface between 5600mm and 5650mm, the darkest crescent is between 6550mm and 6600mm, and the darkest trough between 6600mm and 6650mm, the simulation results can prove that the maze metasurface effectively functions as a lens, concentrating the incoming waves at exactly 1m away, corroborating to researcher's assumption 3.

5. Experiment

5.1. Water wave parameters

The researcher set up the experiment using a bathtub of length approximately 1.20m, width approximately 0.45m, as shown in the following figure. Before the researcher could set out to verify the effectiveness of the metasurface and capture voltage results, the researcher had to determine the parameters of the actual water wave, which cannot be taken for granted.

DOI: 10.54254/2753-8818/2026.HZ30775

Figure 7. Set up of the experiment showing equipment involved in water wave generation itself. (a) a self-assembled Lego structure to create a planar wave, with a linear impact. (b)a miniature reciprocating motor to operate a fixed frequency. (c) an iron rod for the support of the how structure

The researcher inherited the water depth from the simulation section, measuring a depth of approximately 0.2m. A water mark has been used to ensure that the uncertainty from the each filling is kept to a minimum. Using LoggerPro, wavelength of the water wave is approximately 0.0515m, with approximately frequency of 6.14 Hz. The wave speed is 0.316 m/s. (full data is in Appendix 3.) The focus is set 0.4m away from the metasurface. The maze structure was designed similarly to Section 4. Since the water wave parameters changed, by Equation (8), therefore:

$$0.2094m \equiv 2\pi \tag{11}$$

5.2. Wave lensing and energy harvesting

Following the exact same process described in Section 4, part 1, attuning to the newly measured water wave parameters and focal distance of 0.4 m. The following figure shows the structure and the dimensions of the design, consisting of four units symmetrical about a central axis.

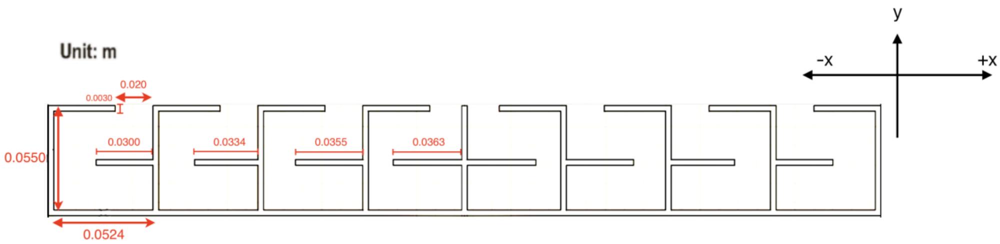

Figure 8. The design for the maze metasurface based on experimental water wave parameters

Since the depth of the water is set at approximately 0.2m, and that water waves only propagate along the surface, the structure have to be higher than the water surface to completely prevent waves from bypassing its structure. Therefore, the structure is 0.25m of height, in z-direction.

3D printing by Polyethylene Terephthalate Glycol (PETG) plastic is used.

DOI: 10.54254/2753-8818/2026.HZ30775

(a) Top view (xy plane) (b) Side view (xz plane)

Figure 9. The real-life representation of the metasurface

However, PETG is low in density, causing it to float. In order to solve that, the researcher planted heavy weights to stabilise it.

Figure 10. The setup with plastic metasurface

The black curves denote the wave plane of reflected water waves, while the blue lines denote the incoming water waves. (They are determined based on the wide base of the wavefront.)

To quantify the results of the experiment , the wave source is structured to be further from the metasurface, so that the wave source is not between the focal point and the meta-surface,though the focus and the wave source are still fairly close to each other. In order to eliminate the effects of amplification of waves near the wave source, the researcher did a control group to illustrate the effectiveness of the lens.

6. Results

For the emphasis of the success of the metasurface, in achieving the purpose of wave focusing, a control group has been used, as shown in figure 11. As suggested in figure 11(b), the focal point is between the wave source and the metasurface, located near where PENG is located. As a control group, the two positions of the peizoelectric nanogenerator are approximately equidistant by eye relative to the wave source, as a controlled variable.

DOI: 10.54254/2753-8818/2026.HZ30775

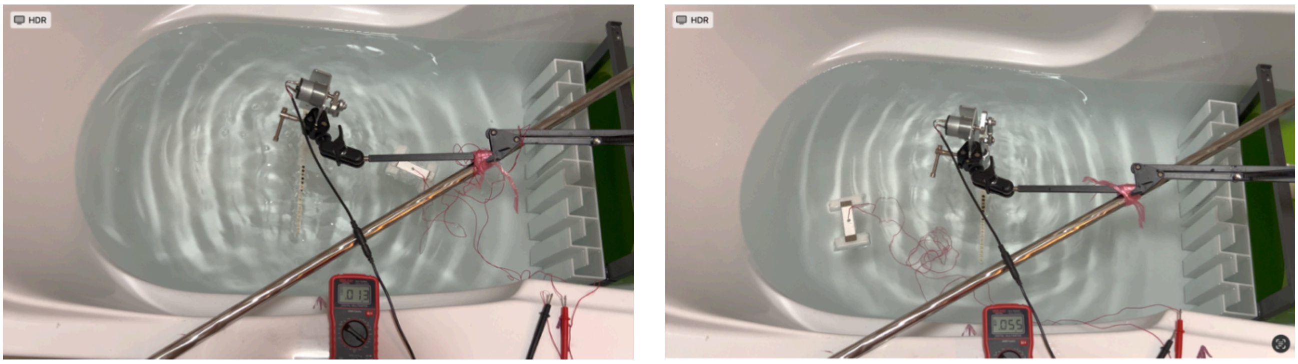

(a) The setup for the experiment. (A)

(b) The setup for the control group. (B)

Figure 11. The contrast of the experimental group and its control

Through video capture per frame, the researcher recorded that the range of the data in the following table. (The video captures are included in Appendix 4)

Table 3. Collection of processed data by video capture

	Min (V)	Max (V)	Range (V)	Time of min (s)	Time of max(s)	Time difference (s)
(A)	-0.056	-0.054	0.002	05.103	04.986	0.117
(B)	-0.038	0.049	0.087	07.055	07.188	0.133

As according to assumption 2 in section 5, the measured frequency of the water waves is approximately 6.14 Hz, i.e. a time period of 0.0163s. Since the time interval between two adjacent maximum (crescent) and minimums (troughs) is half the period, it should be theoretically different by 0.0814s, which is approximately 0.1s.

The last column of table, time difference, appropriates to this value if taken to one significant figure. Therefore, there is significant amplification of the waves near the focal point, producing a voltage that is 43 times larger. This conclusion upholds the practicability of using the experiment to generate effective substantial produces. (This number may be an exaggeration, due to various factors to be discussed in section 7)

7. Discussion

As a reiteration, the assumed distance between the metasurface and the focal point is 0.4m. Yet as shown in figure 8, the distance is approximately 0.6m.The researcher attributed such an error to the sequence along the y axis in which the wave source, the focal point and the metasurface are situated.

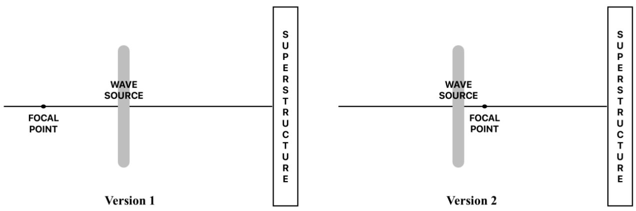

Figure 12. A relative position of the wave source, focal point, and the superstructure. (not to scale)

DOI: 10.54254/2753-8818/2026.HZ30775

However, since after the adjustment, the focal point is actually closer to the wave source than it previously was, making it hard to observe an explicit curvature from the patterns casted by the shadows of water waves. This was slightly troublesome as it impedes the visual element to the verification of the experiment, making the effects much less directly observable. However, the researcher should justify that this does not defeat the validity of the entire design of the experiment, for quantitative results can be cited. To begin with, through data, it is easy to see the metasurface indeed works to significant concentrate the waves.

Apart from experiment, COMSOL simulation results can also exonerate the design of the experiment.

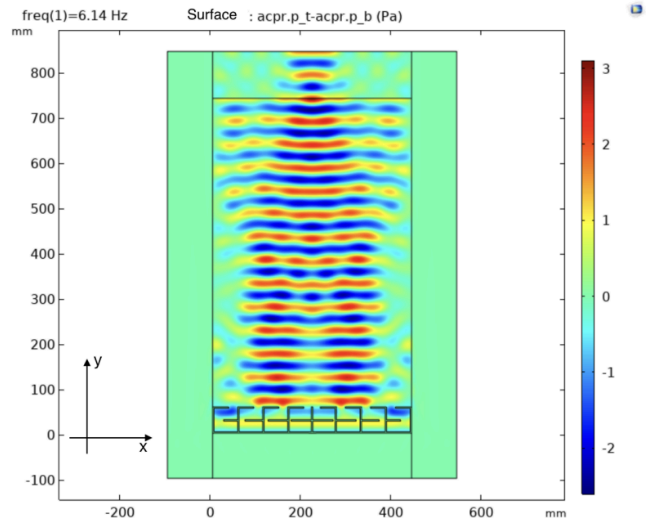

Figure 13. Simulation from COMSOL run with water parameters based on experimental results

Though this is not as perfect as the conditions used purely for simulation purposes, as described in section 4, one can observe as well as a near-rhombus shaped focusing effect at approximately y=400mm.

To conclude, though difficult to spot a focus, it is generally not to be challenged that the metasurface does help significantly in focusing the waves, and achieving so at a largely, predetermined distance.

7.1. Displacement of PENG

As suggested in the title, PENG, be it simply afloat on the water surface, gets pushed outwards rapidly once the motor is started. The researcher believes the errors could be sharply reduced if PENG can be fixed to the bottom of the bathtub. Should time of the project permit, the researcher would be motivated to see to improving that.

Another implication of this displacement is that it may cause exaggeration on the amplification effects of the metasurface itself, as signposted in section 6. As determined by LoggerPro, when the control group was screenshot, PENG is approximately 270mm away from the centre of the wave source, whereas the actual experimental data is taken approximately 200mm away from the centre of the wave source.

DOI: 10.54254/2753-8818/2026.HZ30775

8. Conclusions and future prospects

In summary, this project has achieved effective water wave energy harvesting with the installation of a metasurface structure and a PENG. The mechanism of water wave manipulation by metasurface is first understood by theoretically deriving the externed Snell's law. A mathematical model is also established to design a maze-like metasurface structure, whose functionality is confirmed by finite-element analysis by COMSOL. The designed metasurface is produced by 3D-printing, to further test out its effect in water wave focusing in a bathhub. A maximum voltage of 87 mV has been collected by the PENG with a water frequency of 6.14 Hz, demonstrating a 43 times increase compared with the controlled group. A novel metasurface structure with gradient water depth was further proposed and designed to reduce the reflective loss.

This work has provided a new and feasible method for water wave energy harvesting. Such an innovation is superior to existing water water energy harvesting technology in its effective focusing of wave energy, thereby remarkably enhancing the harvesting efficiency. Further research will be conducted using the new metasurface structure with gradient water depth, as proposed in discussion section. The researcher is also seeking for opportunities for conducting an onsite test at the riverbank to push forward this new technology into real application.

References

[1] UNITED NATIONS. (2025). Ensure access to affordable, reliable, sustainable and modern energy, https: //www.un.org/sustainabledevelopment/energy/

[2] IEA (2025), Global Energy Review 2025, IEA, Paris https: //www.iea.org/reports/global-energy-review-2025, Licence: CC BY 4.0

[3] IEA (2024), Renewables 2024, IEA, Paris https: //www.iea.org/reports/renewables-2024, Licence: CC BY 4.0

[4] UNITED NATIONS. (2018).Tsunami Has Caused $280 Billion in Economic Losses Over the Past Two Decades.https: //news.un.org/zh/story/2018/11/1022022

[5] Xiaoling Tao. (2019). Waves Are the Nemesis of Navigation. https: //aoc.ouc.edu.cn/2019/0627/c15171a251062/page.psp

[6] Zhu, S., Zhao, X., Han, L., Zi, J., Hu, X., & Chen, H. (2024). Controlling water waves with artificial structures. Nature Reviews Physics, 6(4), 231-245.

[7] Cummer, S. A., Popa, B. I., Schurig, D., Smith, D. R., & Pendry, J. (2006). Full-wave simulations of electromagnetic cloaking structures. Physical Review E—Statistical, Nonlinear, and Soft Matter Physics, 74(3), 036621.

[8] Farhat, M., Enoch, S., Guenneau, S., & Movchan, A. B. (2008). Broadband cylindrical acoustic cloak for linear surface waves in a fluid. Physical review letters, 101(13), 134501.

[9] Chen, H., & Chan, C. T. (2008). Electromagnetic wave manipulation by layered systems using the transformation media concept. Physical Review B—Condensed Matter and Materials Physics, 78(5), 054204.

[10] Chen, H., Yang, J., Zi, J., & Chan, C. T. (2009). Transformation media for linear liquid surface waves. Europhysics Letters, 85(2), 24004.

[11] Wang, Z., Zhang, P., Nie, X., & Zhang, Y. (2014). Focusing of liquid surface waves by gradient index lens. Europhysics Letters, 108(2), 24003.

[12] Lan-Hua, Z., Fu-Gen, W., & Hui-Lin, Z. (2010). Effects of orientation and shape of holes on the band gaps in water waves over periodically drilled bottoms. Chinese Physics B, 19(2), 020301.

[13] J. Yang, Y. F. Tang, C. F. Ouyang, X. H. Liu, X. H. Hu, J. Zi; Observation of the focusing of liquid surface waves. Appl. Phys. Lett. 31 August 2009; 95 (9): 094106.

[14] Sun, H. T., Cheng, Y., Wang, J. S., & Liu, X. J. (2015). Wavefront modulation of water surface wave by a metasurface. Chinese Physics B, 24(10), 104302.

[15] Soliman, S. E., Barlou, M., Wong, Z. J., & Tsakmakidis, K. L. (2025). Topological rainbow trapping. Nature Reviews Physics, 1-16.

[16] Li, C., Xu, L., Zhu, L., Zou, S., Liu, Q. H., Wang, Z., & Chen, H. (2018). Concentrators for water waves. Physical Review Letters, 121(10), 104501.

[17] Sadeghi, M. M., Li, S., Xu, L., Hou, B., & Chen, H. (2015). Transformation optics with Fabry–Perot resonances Scientific Report, 5, 8680.
[18] Bobinski, T., Eddi, A., Petitjeans, P., Maurel, A., & Pagneux, V. (2015). Experimental demonstration of epsilon-near-zero water waves focusing. Applied Physics Letters, 107(1).
[19] Pendry, J. B., Martin-Moreno, L., & Garcia-Vidal, F. J. (2004). Mimicking surface plasmons with structured surfaces. Science, 305(5685), 847-848.
[20] Soliman, S. E., Barlou, M., Tsakmakidis, K. L., & Wong, Z. J. (2025). Rainbow trapping for advanced wave control. Advances in Physics: X, 10(1), 2517551.
[21] Archer, A. J., Wolgamot, H. A., Orszaghova, J., Bennetts, L. G., Peter, M. A., & Craster, R. V. (2020). Experimental realization of broadband control of water-wave-energy amplification in chirped arrays. Physical Review Fluids, 5(6), 062801.
[22] Huang, C. T., Song, J., Lee, W. F., Ding, Y., Gao, Z., Hao, Y., ... & Wang, Z. L. (2010). GaN nanowire arrays for high-output nanogenerators. Journal of the American Chemical Society, 132(13), 4766-4771.
[23] LU Z, SHANG J, LUO Z, ... 2018. Experimental Research on the Characteristic of a Generator Used in Wave Energy Conversion [J/OL]. IOP Conference Series: Materials Science and Engineering, 301: 012095 [2025-09-11]. https: //www.researchgate.net/publication/323158007_Experimental_Research_on_the_Characteristic_of_a_Generator_Used_in_Wave_Energy_Conversion.Lu, M. Y., Song, J., Lu, M. P., Lee, C. Y., Chen, L. J., & Wang, Z. L. (2009). ZnO− ZnS heterojunction and ZnS nanowire arrays for electricity generation. ACS Nano, 3(2), 357-362.
[24] Kang, J. H., Jeong, D. K., Ha, J. S., Lee, J. K., & Ryu, S. W. (2017). Enhanced performance of a GaN piezoelectric nanogenerator with an embedded nanoporous layer via the suppressed carrier screening effect. Semiconductor Science and Technology, 32(2), 025001.
[25] Son, M., Jang, H., Lee, M. S., Yoon, T. H., Lee, B. H., Lee, W., & Ham, M. H. (2018). Flexible Transparent Nanogenerators Utilizing Shape-Modulated ZnO Nanorod Arrays on Graphene Electrodes. Advanced Materials Technologies, 3(4), 1700355.
[26] Kanik, M., Aktas, O., Sen, H. S., Durgun, E., & Bayindir, M. (2014). Spontaneous high piezoelectricity in poly (vinylidene fluoride) nanoribbons produced by iterative thermal size reduction technique. ACS Nano, 8(9), 9311-9323.
[27] Jin, Q., He, J., Wang, Z., & Guo, M. (2023, August). The Anomalous Reflection and Refraction of Metasurface in the View of Solar Concentrators. In Journal of Physics: Conference Series (Vol. 2563, No. 1, p. 012028). IOP Publishing.
[28] Chen, H., Chan, C. T., & Sheng, P. (2010). Transformation optics and metamaterials. Nature Materials, 9(5), 387-396.
[29] Zhou, Y. S.; Li, S.; Niu, S.; Wang, Z. L. Effect of Contact- and Sliding-Mode Electrification on Nanoscale Charge Transfer for Energy Harvesting. Nano Research 2016, 9, 3705−3713.
[30] Wang, Z. L.; Wang, A. C. On the Origin of Contact-Electrification. Mater. Today 2019, 30, 34−51
[31] 19 WANG ZL, SONG J. Piezoelectric nanogenerators based on zinc oxide nanowire arrays LJ_. Science, 2006, 312(5771) : 242-246.
[32] Hu, X., & Chan, C. T. (2005). Refraction of water waves by periodic cylinder arrays. Physical Review Letters, 95(15), 154501.